Exploration of Digestive Diseases

Open Exploration

Open Access Review

Monitoring the hepatobiliary function using image techniques and labeled cholephilic compounds

Beatriz Sanchez de Blas[1], Alvaro G. Temprano[1,2], Jose J. G. Marin[1,2], Marta R. Romero[1,2]*

[1]Experimental Hepatology and Drug Targeting (HEVEPHARM), University of Salamanca, Institute for Biomedical Research of Salamanca (IBSAL), 37007 Salamanca, Spain

[2]Centro de Investigación Biomédica en Red de Enfermedades Hepáticas y Digestivas (CIBERehd), Carlos III National Institute of Health, 28029 Madrid, Spain

***Correspondence:** Marta R. Romero, Experimental Hepatology and Drug Targeting (HEVEPHARM), University of Salamanca, Institute for Biomedical Research of Salamanca (IBSAL), Campus Miguel de Unamuno, ED-Lab 118, Plaza Doctores de la Reina, 37007 Salamanca, Spain. marta.rodriguez@usal.es

Academic Editor: Agustín Albillos, University of Alcalá, Spain

Received: July 28, 2022 **Accepted:** October 11, 2022 **Published:** February 28, 2023

Cite this article: de Blas BS, Temprano AG, Marin JJG, Romero MR. Monitoring the hepatobiliary function using image techniques and labeled cholephilic compounds. Explor Dig Dis. 2023;2:18–33. https://doi.org/10.37349/edd.2023.00015

Abstract

Evaluation of the hepatobiliary function is critical for the clinicians, not only for the diagnosis of a large variety of liver diseases but also in the follow-up and management of some patients, for instance, those with different degrees of cholestasis suffering from a drug-induced liver injury (DILI) or scheduled for liver resection. Currently, the determination of global liver function mainly relies on laboratory tests, clinical scores, and data from images obtained with ultrasonography, computed tomography (CT), or magnetic resonance. Nuclear medicine scanning, displaying either planar or three-dimensional spatial distribution of liver function, is enhanced when using hepatotropic tracers based on classical radioisotopes such as technetium-99m (^{99m}Tc) and with higher resolution using metabolized probes such as those based on monosaccharide derivatives labeled with ^{18}F. Other cholephilic compounds, and hence selectively secreted into bile, have been proposed to visualize the correct function of the liver parenchyma and the associated secretory machinery. This review aims to summarize the state-of-the-art regarding the techniques and chemical probes available to monitor liver and gallbladder function, in some cases based on imaging techniques reflecting the dynamic of labeled cholephilic compounds.

Keywords

Bile, bile acid, cholephilic compounds, cholestasis, liver failure, transport

Introduction

Evaluation of the hepatobiliary function is often required in clinical practice, not only for the diagnosis of different liver diseases, such as cholestasis and drug-induced liver injury (DILI), but also for the assessment of oncological and intensive care patients, and especially for those scheduled for liver resection, since in this

group of patients, liver failure has remained a major cause of mortality after hepatectomy, which implies that a close follow-up is recommended.

The use of omics techniques has made it possible to screen the changes in circulating metabolites with the intention of using them to monitor liver function. Thus, although non-alcoholic fatty liver disease (NAFLD) is one of the most common liver disorders worldwide, and its early diagnosis is critical, there is a lack of reliable biomarkers for diagnosis, prognosis, and monitoring of disease progression and response to treatment. In this regard, some progress has been made in the characterization of metabolomic and lipidomic profiles to identify biomarkers associated with both NAFLD and non-alcoholic steatohepatitis (NASH), which, upon validation, could be used as biomarkers in noninvasive diagnostic tests in the clinical practice in the near future [1]. In more general terms, the determination of liver function is currently primarily based on laboratory tests that include the measurement of serum biomarkers, such as albumin, alkaline phosphatase (ALP), bilirubin, gamma-glutamyl transferase (GGT), prothrombin time (PT), and transaminases [alanine transaminase (ALT) and aspartate transaminase (AST)] [2].

However, despite their popularity, these biomarkers lack specificity because their serum levels are elevated in a broad panel of liver diseases. Therefore, to get an overall estimation of the degree of impairment in liver function, several clinical scores have been proposed. Two commonly used scores are Child-Pugh, which includes the presence of ascites, serum levels of albumin and total bilirubin, PT, and signs of hepatic encephalopathy [3], and the model for end-stage liver disease (MELD), commonly used to evaluate the liver function of patients in the waiting list for liver transplantation [4].

The tests mentioned above and clinical scores are minimally invasive, and they can be helpful together with other diagnostic approaches that generate data from images obtained with ultrasonography, computed tomography (CT), or magnetic resonance imaging (MRI) (Table 1).

Table 1. Image techniques commonly used to assess the liver structure and function

Liver pathology	Image techniques	Alternatives	References
Biliary leak	Cholescintigraphy	NA	[5]
Gallstones	ERCP	PTC	[6, 7]
Cholecystitis	Cholescintigraphy	NA	[8, 9]
Cholestasis	Cholescintigraphy	PET-CT	[8, 10]
Hepatic fibrosis	Ultrasound elastography	MRI, MRE	[11–16]
Liver cancer	Ultrasonography	CT/MRI	[13, 17]
Liver metastasis	MRI/CT	NA	[15, 18]
Liver steatosis	Ultrasonography	NA	[12]
Obstructed/dilated ducts	Cholescintigraphy	NA	[19, 20]

ERCP: endoscopic retrograde cholangiopancreatography; MRE: magnetic resonance elastography; NA: none available; PET: positron emission tomography; PTC: percutaneous transhepatic cholangiography

Some alternative tests used in liver function evaluation are classical, such as these performed using hepatotropic agents, i.e., efficiently accumulated by the liver or cholephilic compounds, i.e., substances in most part taken up by the liver and secreted into bile. A significant limitation in using these agents to estimate whole liver function is that most of them are not homogeneously distributed throughout the hepatobiliary system.

A more recently incorporated assay is the "liver maximum function capacity (LiMAx)" test [21]. In this assay, a real-time liver function evaluation is carried out by determining liver-specific CYP1A2-mediated metabolism of ^{13}C-methacetin to paracetamol and $^{13}CO_2$, which is measured in the exhaled air within 20–30 min after the intravenous injection of the substrate (^{13}C-methacetin). Even though LiMAx test is becoming commonly used, it cannot provide the regional distribution of dysfunctional hepatocytes in the liver. Localizing the areas with impaired liver function is clinically relevant, for instance, before liver resection [22]. To overcome this limitation, it is necessary to use different high-resolution images, either planar or three-dimensional, which permits more accurate regional information. In this respect, scintigraphy, MRI, or single-photon emission (SPE)-CT with, among others, technetium-99m (^{99m}Tc)

classical tracers and with gadolinium ethoxybenzyl (Gd-EOB) for an enhanced resolution are currently used in clinical practice.

This review aims to summarize the state-of-the-art regarding the techniques and chemical tools available to monitor liver and gallbladder function, in some cases based on imaging techniques reflecting the dynamic of hepatotropic and cholephilic labeled compounds.

Imaging techniques in the analysis of the hepatobiliary

Ultrasonography

Ultrasonography is the most sensitive and the least expensive procedure for providing structural information of the biliary system [11], which makes it the technique of choice for the screening of biliary tract abnormalities, evaluating right upper quadrant abdominal pain, screening for liver masses, differentiating intra- from extrahepatic causes of jaundice and the diagnosis of liver steatosis [12]. Ultrasonography can also be used to detect splenomegaly, which may suggest a diagnosis of portal hypertension.

Transabdominal ultrasonography is helpful in detecting focal liver lesions such as cysts over 1 cm in diameter because, in general, they are echo-free, but also tumors or abscesses that are usually echogenic. In patients at a high risk of hepatic fibrosis or liver cancer, i.e., hepatocellular carcinoma (HCC), early detection and stratification of primary and metastatic lesions could be done with ultrasonography. In general, this technique can be helpful in selecting the most effective treatments in some cases, such as chronic hepatitis B and C, hemochromatosis, and liver cirrhosis [13].

The assessment of hepatic fibrosis can be carried out by ultrasound elastography, a procedure where the vibration emitted by a transducer induces an elastic shear wave. The rate of the speed at which the wave is propagated through the liver is proportional to the stiffness of the tissue [11, 14].

Cholescintigraphy

This technique requires using radiotracers to assess the anatomy and function of the biliary system. This approach is sensitive and specific for detecting biliary leaks. Cholescintigraphy is usually carried out with ^{99m}Tc-labeled iminodiacetic acid (IDA) derivative, which justifies its acronym of hepatobiliary IDA (HIDA) scan. The technique is also called hepatobiliary scintigraphy (HBS) [8, 9].

Cholescintigraphy is highly helpful for the diagnosis of acute cholecystitis [5]. When the gallbladder is not filled with the radionuclide imaging agents or there is a decreased clearance of the radiotracer, a functional obstruction of the cystic duct, acute cholecystitis cholestasis, and/or hepatocyte dysfunction can be diagnosed.

Furthermore, cholescintigraphy can supply valuable diagnostic information in patients with complications after laparoscopic, partial hepatic resection [19, 20, 23], or liver transplantation. Moreover, it is the only extracorporeal method to distinguish between chronically dilated ducts, obstructed dilated ducts, and chronically dilated but not obstructed ducts. Moreover, since the tumoral liver cells are hypofunctional compared to normal hepatocytes, cholescintigraphy can help in the diagnosis of more and less differentiated (benign and malignant, respectively) liver tumors. In patients with impaired liver function after a chemotherapy treatment, HIDA scan has been reported to be the best choice to assess the intrahepatic regional distribution of liver function [24].

CT

CT has been commonly performed for several years to assess the integrity of the hepatobiliary system. This imaging technique is one of the preferred methods because it supplies the clinician with excellent images of the liver and also valuable information on the state of intrahepatic blood vessels. CT is particularly useful for detecting biliary tract abnormalities and various liver disorders, including abscesses, fat accumulation in liver parenchyma, inflammation, and tumors [25–27]. During the procedure, part of the equipment consisting of an X-ray source and X-ray detector rotates around the patient, taking data from multiple angles, which are

converted by a computer into images that mimic 2-dimensional or 3-dimensional slices of the scanned region of the body [28].

Currently, there are different available variants of CT, i.e., SPE-CT, dual-energy CT (DECT), and metabolic imaging with PET-CT [29, 30]. Compared with single-detector CT, multidetector CT (MDCT) is superior due to higher speed, thinner slices, and multiphasic scanning; these factors enhance spatial and temporal resolution, providing a more precise evaluation of liver tumor hemodynamics. Consequently, they result in enhanced diagnostic accuracy [31]. CT is used as a second-line diagnostic imaging modality in clinical practice because it has some drawbacks, such as patient exposure to ionizing radiation, the need for anesthesia, and its limited availability. Accordingly, CT is usually performed to confirm the presence of primary HCC lesions and determine their size and stage [17], after this has been suggested by other commonly used diagnostic tests, such as serum alpha-fetoprotein levels and ultrasonography.

MRI

MRI is a radiological diagnostic modality that uses radio waves and strong magnetic fields [32]. Diffusion-weighted (DWI)-MRI resembles its image contrast from divergences in the movement of H_2O molecules between tissues which correlates inversely with the cell membrane and tissue integrity. Thus, this movement is more restricted in tissues with high intact cell membranes and increased cell density (i.e., tumor masses). The advantages of DWI-MRI include the absence of ionizing radiation emission and that there is no need to use paramagnetic contrast, which implies that the study can be performed even in patients with impaired kidney function [32]. Dynamic contrast-enhanced (DCE)-MRI is potentially useful for characterizing the angiogenic activity of liver cancer and metastases, which makes it helpful in supervising antiangiogenic therapy response and in the diagnosis of advanced liver fibrosis and cirrhosis [15].

MRE, a phase contrast-based MRI modality, has become of clinical importance in the diagnosis, and staging of liver fibrosis, being a complementary approach to the analysis of liver stiffness evaluation by ultrasonography [16]. Although the latter has the added advantage of lower cost and accessibility, ultrasonography has lower accuracy and reliability than MRE [33].

Cholangiography

ERCP is a diagnostic and therapeutic technique for the detection of biliary strictures [34], tissue sampling, and effective removal of gallstones located in the extrahepatic biliary tree [6]. ERCP is widely available and has a relatively low complication rate but sometimes fails due to anatomic alterations or technical problems. In these cases, the alternative is either to perform endoscopic ultrasound-guided biliary drainage (EUS-BD) [35] or percutaneous transhepatic biliary drainage (PTBD) [36]. However, the latter is associated with a high rate of complications, accounting for higher mortality [35].

PTC is a minimally invasive approach used to evaluate the degree and treatment of obstructions of the biliary tract and nearby tissues. Using ultrasound or fluoroscopy, this technique generates an image after the injection of contrast dye into the bile duct [6, 7]. However, PTC could involve a few adverse events such as temporary biloma, hemobilia, and bile leakage [37–39] that usually resolve spontaneously and do not result in more severe conditions.

Since ERCP and PTC permitted biopsy and cytology sampling, both techniques are sensitive and accurate for diagnosing malignant biliary strictures. However, the latter is a better option for masses located in the hilum [6]. Nevertheless, ERCP provides higher accuracy and sensitivity than PTC for strictures located in the lower segment of the common bile duct. EUS-BD and PTC are equally effective, but EUS-BD seems safer in patients with malignant biliary strictures who have undergone a failed procedure of ERCP [40].

Intraoperative cholangiography (IOC) is sometimes performed during a cholecystectomy [41]. This is carried out by placing a catheter into the cystic duct, which is followed by a dye injection and draining the bile from the gallbladder into the common bile duct. The technique permits to taking of X-rays images for diagnostic purposes. This method provides a view of the biliary system anatomy, which helps identify choledocholithiasis and may significantly impact the details of a surgical approach as well as the postoperative

management of the patient [42]. However, according to a recent meta-analysis [43], IOC offers a poorer visualization of the cystic and common hepatic ducts compared to fluorescence cholangiography. Accordingly, the latter can be considered a better choice to visualize the extrahepatic biliary tree and improve patient outcomes during cholecystectomy.

Tracer compounds for hepatobiliary function evaluation

Several probes are used in image techniques because they are accumulated in the liver due to the fact that they are hepatotropic, i.e., efficiently taken up by the liver, or their hepatocyte-specific metabolism favors enhanced concentrations of these compounds or their derivatives in the liver. In the case of probes used for the detection of liver cancer and its metastasis, their accumulation is not liver-specific but associated with characteristics of cancer tissue metabolism. Another group of probes is constituted by cholephilic compounds, i.e., they are selectively taken up by hepatocytes and actively secreted into bile.

Probes based on ^{99m}Tc

This γ-emitting radionuclide is used in planar scintigraphy and PET-CT due to its ideal nuclear properties for optimal imaging using γ-cameras. Depending on the target, a broad spectrum of different ligands has been bonded to ^{99m}Tc (e.g., propylene amine oxime ligands, mixed and bidentate ligands, and carboranes). Moreover, new derivatives have been obtained linking ^{99m}Tc to proteins, macromolecules, and nanoparticles [44].

To quantitatively assess liver function, many ^{99m}Tc compounds have been developed (Figure 1). Among them, the most commonly used are ^{99m}Tc-IDA and ^{99m}Tc-mebrofenin (Figure 1A), as well as ^{99m}Tc-labeled galactosyl human serum albumin (^{99m}Tc-GSA) (Figure 1B) [44, 45] and ^{99m}Tc-mebrofenin human serum albumin (^{99m}Tc-MHSA) [46]. Dynamic ^{99m}Tc-GSA and ^{99m}Tc-MHSA scintigraphy combined with SPE-CT permits the acquisition of 3 dimensions useful in the analysis of liver function. This imaging approach gives qualitative and quantitative information on hepatic drug uptake and biliary excretion. It has been reported that only hepatocytes are able to take up ^{99m}Tc-GSA and are not affected by biliary tract obstruction, permitting its direct use in the exploration of the hepatobiliary secretory pathway in patients with cholangiocarcinoma (CCA) and HCC [45]. However, only ^{99m}Tc-IDA (Figure 1A) using SPE-CT is currently the imaging-based hepatocellular function test used to diagnose various hepatobiliary pathologies, including primary biliary cirrhosis, acute hepatitis, and jaundice, among others [47]. For these purposes, many IDA derivatives have been synthesized [48].

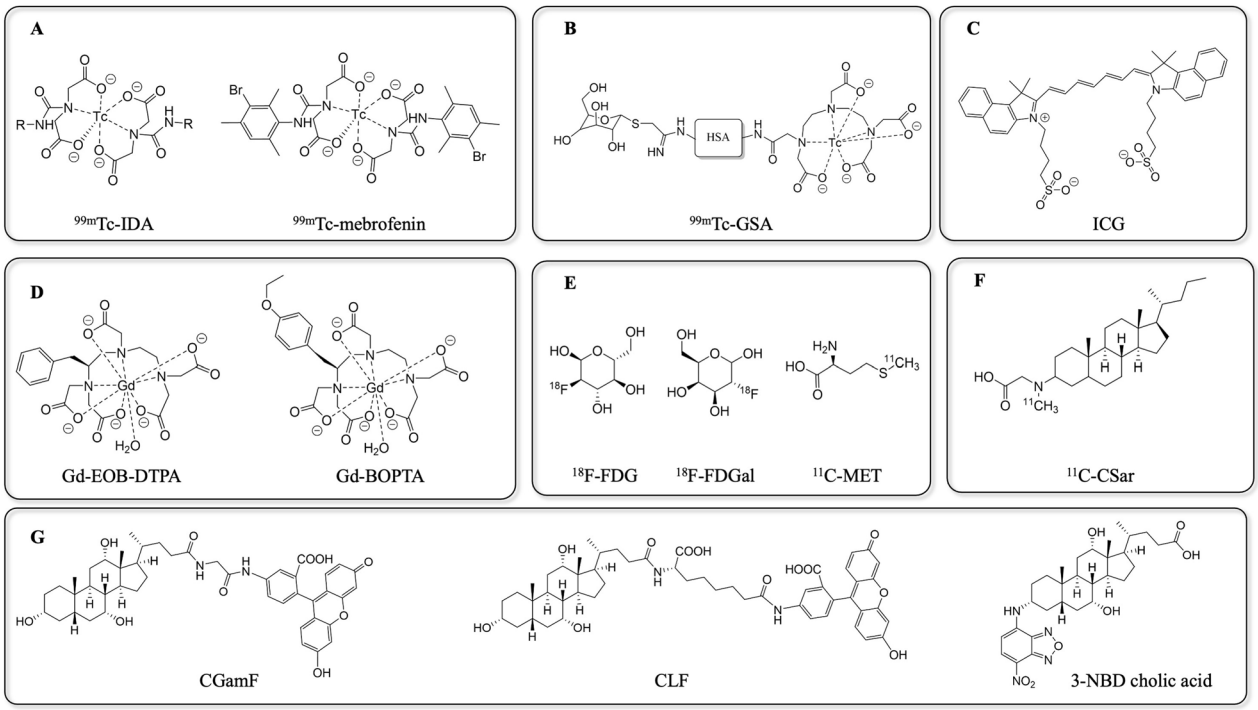

Figure 1. Radiotracers and fluorescent probes commonly used in clinic and in preclinical assays of liver and gallbladder function. ^{11}C-CSar: *N*-methyl-^{11}C-cholylsarcosine; ^{11}C-MET: ^{11}C-methionine; ^{18}F-FDG: 2-[^{18}F]fluoro-2-deoxy-*D*-glucose; ^{18}F-FDGal: 2-[^{18}F]

fluoro-2-deoxy-*D*-galactose; CGamF: cholyl-glycylamido-fluorescein; CLF: cholyl-*L*-lysyl-fluorescein; Gd-BOPTA: gadobenate dimeglumine; Gd-EOB-DTPA: gadolinium ethoxybenzyl diethylenetriamine pentaacetic acid; HSA: human serum albumin; ICG: indocyanine green; NBD: nitrobenzoxadiazole

Probes based on gadolinium

As mentioned above, MRI is a powerful medical diagnostic tool whose efficiency is greatly improved by using contrast agents (CAs). The most used CA is gadolinium (Gd), a lanthanide ion with seven unpaired electrons. Its popularity is due to its efficiency in enhancing proton relaxation because of its high magnetic moment and paramagnetic properties. Moreover, Gd can coordinate water efficiently. However, Gd is toxic due to its calcium-antagonistic activity. To prevent its toxicity, Gd is chelated with specific interacting structures, such as linear multifunctional or macrocycle compounds [49]. For instance, Gd-EOB-DTPA or disodium gadoxetate (Figure 1D) is commonly used as a liver-specific CA for MRI imaging because healthy hepatocytes can take it up efficiently. The compound is secreted into bile 10–20 min after injection. Several studies have demonstrated that MRI using Gd-EOB-DTPA provides diagnostic accuracy for liver lesions and HCC [50, 51]. However, it is essential to take into account that genetic polymorphisms affecting liver transporters for organic anions [organic anion transporting polypeptides (OATPs)] (Figure 2), as well as some drug interactions, can decrease Gd-EOB-DTPA uptake by hepatocytes. This impairs the visualization of focal liver lesions and may lead to a misinterpretation of liver images, limiting, therefore, the diagnostic value of this tracer [52].

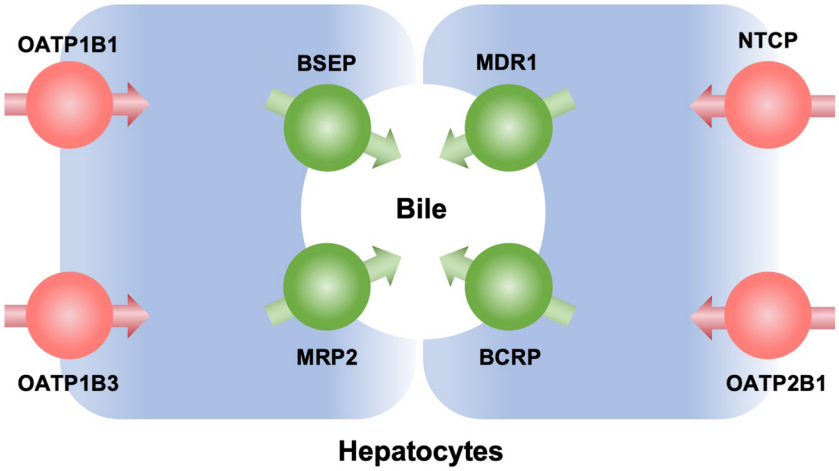

Figure 2. Main transporters involved in hepatocyte uptake and secretion into bile of probes used to evaluate hepatobiliary function. BCRP: breast cancer resistance protein; BSEP: bile salt export pump; MDR1: multidrug resistance protein 1; MRP2: multidrug resistance-associated protein 2; NTCP: Na^+-taurocholate co-transporting polypeptide

Besides, Gd-BOPTA (Figure 1D) also enhances the accuracy of liver MRI and hence is used to acquire quantitative and visual information on liver morphology to evaluate hepatic fibrosis and hepatitis [53]. Gd-BOPTA specificity as a liver-tracer is due to the ability of OATP1B1 (gene *SLCO1B1*) and OATP1B3 (gene *SLCO1B3*) (Figure 2) to transport this compound and hence favor its uptake by hepatocytes. The tracer is subsequently secreted into bile 40–120 min after administration [54].

Probes based on carbohydrate metabolism

Exacerbated glucose metabolism in neoplastic tissue has been used to develop probes to label tumor lesions in the liver. Thus, ^{18}F-FDG PET-CT (Figure 1E) has been used in clinical practice to detect liver metastases with high accuracy [18]. This probe has also been useful in staging the tumors and monitoring therapy response in several liver cancers, such as HCC, CCA, and gallbladder cancer [55, 56]. In addition, ^{18}F-FDG is also helpful in combination with MRI in the follow-up of neoplastic liver lesions [57–62] and detects recurrency in a wide variety of malignancies [63, 64].

Besides, PET-CT with the liver-specific galactose tracer ^{18}F-FDGal permits quantifying hepatic metabolic function [65, 66]. During tumor development, some changes in cancer cell metabolism occur, which can be detected before morphological changes can be observed with CT or MRI. Consequently, PET-CT with ^{18}F-FDGal has been extensively used for diagnosing and staging a wide variety of cancers. Nevertheless, although

^{18}F-FDGal is the most used PET probe for diagnosing liver diseases, the sensitivity of ^{18}F-FDG detection by PET-CT in HCC is low [67, 68]. Despite this limitation, ^{18}F-FDGal plus PET-CT may contribute to the diagnosis of HCC and has potential clinical usefulness for detecting extra and intrahepatic HCC nodules [69–71]. Indeed, ^{18}F-FDGal has proven helpful to detect extrahepatic metastases in patients diagnosed with HCC. The use of PET/CT with ^{18}F-FDGal gives better results than a standard clinical examination with contrast-enhanced CT and/or MRI. One population in which the use of ^{18}F-FDGal is of particular interest is in patients considered suitable for locoregional treatment because PET/CT with ^{18}F-FDGal can permit the personalized adaption of the initially planned treatment of these patients [71]. Besides liver cancer applications, ^{18}F-FDGal plus PET-CT has been used as a tracer for measuring regional metabolic function noninvasively in patients with cirrhosis [72, 73].

Amino acids have also been used as CAs in PET-CT. This is the case of ^{11}C-MET (Figure 1E), which has been helpful in diagnosing focal lesions in the central nervous system [72, 73], in the assessment of disease activity in multiple myeloma patients [74], and in the determination of hepatic and extrahepatic tumor size in patients with HCC [75]. Moreover, ^{11}C-MET has also been used as a valuable probe in pediatric patients for evaluating malignant diseases in non-tumor-involved organs [76]. Some preliminary studies [77] indicate that PET-CT using ^{11}C-MET is more sensitive for assessing myeloma than ^{18}F-FDG. However, there is no clear evidence regarding its advantage over ^{18}F-FDG in solid tumors [72]. Nevertheless, its sensitivity for HCC seems lower than that of ^{11}C-acetate PET, which also gives information on tumor cell differentiation [56].

The combination of PET with [*N*-methyl-^{11}C]-choline (^{11}C-choline) has been explored as a tool in the detection of well-differentiated HCC, which was based on the differential relationship between uptake and metabolism in cancer and healthy liver tissue. Studies in animal models of HCC using woodchucks revealed that this tumor exhibits increased uptake of ^{11}C-choline, whereas this is only moderate in surrounding liver tissues. In HCC, there is an initial enhancement in ^{11}C-choline uptake due to active transport and phosphorylation; however, over time, increased radioactivity accumulation is due to the increased incorporation of ^{11}C-choline into the synthesis of phosphatidylcholine. In contrast, in surrounding liver tissues, there is an extensive oxidation of ^{11}C-choline through the phosphatidylethanolamine methylation pathway, which contributes significantly to the observed accumulation of radioactivity in this tissue [78].

Although the use of radiolabeled probes is not exempt from risks, this is clinically acceptable. Indeed, even used at therapeutical doses, the toxicity induced by ^{18}F-FDG, for instance, is limited to acute and reversible mild gastrointestinal and hematological side effects [79].

ICG test

ICG is a hydrophilic tricarbocyanine dye (Figure 1C), which after intravenous injection, rapidly binds to plasma proteins and is secreted by the liver in bile, due to hepatobiliary transporters, such as OATPs [80] and MDR1 (gene *ABCB1*) (Figure 2) [81]. ICG becomes fluorescent when excited by a flash of light in the near-infrared (NIR) spectrum, which can be detected extracorporeally. NIR fluorescence imaging has the advantage over other fluorescent approaches of better tissue penetration. After illumination by a NIR ray, this probe enables real-time intraoperative visualization of superficial lymphatic nodes and vessels transcutaneously. Therefore, NIR fluorescence imaging using ICG has been reported to provide excellent diagnostic accuracy when the aim is to detect sentinel lymph nodes in cancer or visualize microvascular circulation in various ischemic diseases.

The sensitivity using ICG fluorescence is higher than that of radioisotope-based methods [82]. Moreover, the ICG test has been used to assess liver function before surgical tumor removal [83] to identify patients at risk of postoperative liver dysfunction [84, 85]. This can effectively reduce operative time and increases the success of complete tumor resection [86], and decrease postoperative complications [87–89]. ICG is used for routine real-time imaging during clinical exploration, and hepatic resection in HCC allows the identification of superficial tumors and liver resection margins [90]. ICG could also be helpful in identifying metastatic liver tumors [82]. The use of ICG has been explored in other liver tests, such as fluorescent cholangiography (ICG-FC) [43, 91].

Radiolabeled bile acids to test hepatobiliary secretion

Bile acids are molecules with marked hepatotropism due to the selective and efficient plasma membrane transporters expressed in cells of the enterohepatic circuit. More precisely, in hepatocytes, this function is carried out by NTCP (gene *SLC10A1*) and OATPs (Figure 2). This characteristic makes them excellent molecules to be used as drug shuttles directed to target tissues, improving their bioavailability and metabolic stability [92]. Besides, biliary elimination of these drugs is also facilitated by ATP-dependent active transporters, mainly BSEP (gene *ABCB11*) and MRP2 (gene *ABCC2*) (Figure 2) expressed in the canalicular membrane of hepatocytes, preventing the long-term accumulation of bile acids and their derivatives that could cause noxious side effects in healthy cells.

Due to their peculiar structure, bile acids are very versatile building blocks for obtaining semisynthetic compounds. In nature, there are many bile acid molecular species characterized by different functional groups in their steroid ring and the side chain. This implies that pharmacological agents can be attached at different positions of the molecule resulting in a broad range of derivatives. Besides, different types of chemical bonds, spacer lengths, stereochemistry, and polarity can also be used to couple drugs, further increasing the diversity of possible derivatives.

Radiolabeled bile acid tracers have been used in clinical practice to evaluate intrahepatic cholestasis liver disease [10]. Thus, the usefulness of ^{11}C-CSar (Figure 1F) in combination with PET-CT to assess hepatobiliary function is based on the fact that ^{11}C-CSar detection permits determine that its hepatic clearance rate is > 3-fold faster in healthy individuals than in patients with cholestasis. Moreover, this tracer has been used to study the dynamic of bile acid secretion in healthy volunteers at the postprandial state [93]. Other bile acids derivatives conjugated with *N*-[^{11}C]methyl-taurine have been developed but they are yet to be approved for human administration [94].

^{18}F-labeled bile acid tracers have also been synthesized and used in combination with PET-CT. The fluorinated compound ^{18}F-lithocholic acid triazole derivative (LCATD) has been demonstrated to be taken up and secreted by the liver in *in vivo* models. Tracking the probe through the biliary tree is possible from 1–2 min post-injection. After 20 min, the signal is clearly visible in the intestinal region, while almost no radioactivity was already detectable in the liver [95].

Other PET-CT probes based on radioactive bile acids such as cholic, deoxycholic, and chenodeoxycholic acid have been synthesized. These have been obtained by attaching a bifunctional chelate to their side chain (*N*-NE3TA), which is capable of binding ^{64}Cu, an isotope widely used in radiopharmaceutical preparations. However, to date, only their *in vitro* stability in human plasma has been determined. Thus, further studies are needed to elucidate their actual usefulness as tracer molecules to be used in combination with PET-CT [96].

Some radioactive derivatives of bile acids have also been synthesized for the study of specific questions related to bile acid homeostasis. [^{14}C]tauro-lithocholic acid-3-sulfate was synthesized to elucidate substrate specificity of BCRP pump (gene symbol *ABCG2*) present in hepatocytes (Figure 2) and placenta cells. When expressed in frog (*Xenopus laevis*) oocytes, BCRP was able to transport bile acids, which has helped to understand the role of this pump in the placental barrier as an element of fetal protection in cases of maternal hypercholanemia, such as that occurring during intrahepatic cholestasis of pregnancy [97]. Besides, [^{14}C]tauro-*allo*-cholic acid has been helpful in studying the physiological characteristics of "flat" bile acids that reappear during liver regeneration and carcinogenesis [98].

Probes based on fluorescent bile acid derivatives

Side-chain modification of bile acids by binding fluorescent compounds permits to carry out functional *in vitro* and *in vivo* tests to evaluate the function of members of the OATP family of transporters (mainly, OATP1B1 and OATP1B3) and the canalicular efflux transporters BSEP and MRP2, involved in the dynamics of cholephilic compounds [99].

In this sense, CGamF (Figure 1G) is used for studies on bile-acid transport in liver cells [100] and for *in vitro* drug interaction studies [97, 101, 102]. This fluorescent derivative, together with analogs obtained by conjugating different bile acids, such as chenodeoxycholyl-glycylamido-fluorescein (CDCGamF) and

ursodeoxycholyl-glycylamido-fluorescein (UDCGamF), have been used in rat hepatocytes to elucidate the cytosol-nucleus traffic of conjugated bile acids [102]. These studies permitted to visualize the colocalization of bile acids and farnesoid X receptor (FXR) in intranuclear regions identified as nucleoli based on their lower DNA density and enhanced abundance of nucleolin [102].

Moreover, CGamF uptake analysis by immunofluorescence coupled with confocal microscopy has been used as a proof-of-concept for the evaluation of the vectorial ability of bile acid conjugates in drug-targeting by directing antitumor agents towards cancer cells expressing bile acid transporters. For instance, NTCP and OATP1B1/3 in cancer cells derived from hepatocytes in HCC [103] and apical sodium-dependent bile acid transporter (ASBT, gene *SLC10A2*) in cancer cells derived from cholangiocytes in CCA [104].

CLF (Figure 1G) is a fluorescent bile acid derivative analog to CGamF that was synthesized as an alternative probe for determining *in vivo* liver function [105–108] and quantification of the inhibition by drugs of its biliary efflux, which is interesting because similar alteration can occur in patients with DILI [109]. Besides, CLF has been a valuable tool to be used in combination with intravital imaging performed through confocal microscopy in anesthetized mice to study the mechanisms involved in the generation of bile flow [110].

A dansyl-ethylene diamine precursor was linked to the sulfonyl group of taurine. The resulting dansyl-taurine was conjugated to the carboxyl group of free bile acids to obtain five fluorescent cholanoyl derivatives with different hydrophilicity. These fluorescent dansylated bile acid derivatives provide a useful tool for studying the role of amphipathic properties of bile acids in their handling by hepatocytes [111]. Besides, they have been used to investigate the binding behavior of bile acids to proteins and also to study in detail the aggregation properties of bile acids on which many of their physiological functions are based [112].

Derivatives such as chenodesoxycholic pacific blue (CDCenPB), obtained by linking bile acids, in this case chenodesoxycholic acid (CDCA), to the fluorochrome pacific blue (PB), a hydroxycoumarin bearing two fluoro substituents, which emits in the UV-visible range of the spectrum, have also been synthesized. Using *in vitro* models, CDCenPB has been shown to be a suitable substrate for both basolateral transporters OATP1B3 and OATP2B1 (Figure 2), as well as the canalicular membrane export pumps BSEP and MRP2. Accordingly, CDCenPB may be a helpful tool for studying the *in vivo* dynamics of bile acids [99].

Lipids labeled with NBD are commonly fluorescent tracers helpful in assessing membrane composition and dynamics [113]. NBD has also been used to obtain fluorescent bile acids derivatives. Thus, cholic acid has been conjugated with 4-nitrobenzo-2-oxa-1,3-diazole fluorescent at positions 3α, 3β, 7α, and 7β to obtain different diastereomeric compounds. These derivatives have been used for *in vitro* study of bile acid uptake [114]. Using flow cytometry, it is possible to measure the increase of green fluorescence accumulation over time in cells incubated with fluorescent NBD-cholic acid derivatives (Figure 1G) [114]. In addition, the uptake of NBD-bile acids derivatives through bile acid transporters is inhibited by chlorpromazine sodium, valproate, and cyclosporin A. Interestingly, these compounds can induce cholestatic. These results support the usefulness of NBD-bile acids derivatives as potential markers for cholestatic liver diseases.

Conclusions and perspectives

Over the last decades, many complementary techniques to study liver structure and function have been developed, both at the organ level but also at the tissular and cellular levels. Their advantages and drawbacks have been briefly commented on in this review article. Among them, only a few have reached routine clinical practice. Nevertheless, despite their usefulness, none is very specific. Moreover, many of them are invasive, expensive, and not exempt from secondary effects. The critical reading of the available information in this field leads to two important conclusions. On the one hand, the appropriate selection of the approach to be used should be carefully made to get the maximum information with minimal risk for the patient and cost for the healthcare system. On the other hand, the significant limitations of the available tools highlight the need to develop novel approaches to evaluate hepatobiliary function, such as molecules with enhanced hepatotropism and/or biliary secretion and a better safety profile.

Abbreviations

^{11}C-choline: [*N*-methyl-^{11}C]-choline

^{11}C-CSar: *N*-methyl-^{11}C-cholylsarcosine

^{11}C-MET: ^{11}C-methionine

^{18}F-FDG: 2-[^{18}F]fluoro-2-deoxy-*D*-glucose

^{18}F-FDGal: 2-[^{18}F]fluoro-2-deoxy-*D*-galactose

^{99m}Tc: technetium-99m

^{99m}Tc-GSA: technetium-99m-labeled galactosyl human serum albumin

BCRP: breast cancer resistance protein

BSEP: bile salt export pump

CAs: contrast agents

CCA: cholangiocarcinoma

CDCenPB: chenodesoxycholic pacific blue

CGamF: cholyl-glycylamido-fluorescein

CLF: cholyl-*L*-lysyl-fluorescein

CT: computed tomography

ERCP: endoscopic retrograde cholangiopancreatography

EUS-BD: endoscopic ultrasound-guided biliary drainage

Gd: gadolinium

Gd-BOPTA: gadobenate dimeglumine

Gd-EOB-DTPA: gadolinium ethoxybenzyl diethylenetriamine pentaacetic acid

HCC: hepatocellular carcinoma

ICG: indocyanine green

IDA: iminodiacetic acid

MRE: magnetic resonance elastography

MRI: magnetic resonance imaging

MRP2: multidrug resistance-associated protein 2

NBD: nitrobenzoxadiazole

NIR: near-infrared

NTCP: Na^+-taurocholate co-transporting polypeptide

OATPs: organic anion transporting polypeptides

PET: positron emission tomography

PTC: percutaneous transhepatic cholangiography

SPE: single-photon emission

Declarations

Author contributions

BSdB and AGT: Investigation, Writing—original draft. JJGM: Investigation, Supervision. MRR: Investigation, Writing—original draft, Project administration.

Conflicts of interest

The authors declare that they have no conflicts of interest.

Ethical approval

Not applicable.

Consent to participate

Not applicable.

Consent to publication

Not applicable.

Availability of data and materials

Not applicable.

Funding

This study was funded by the CIBERehd [EHD15PI05/2016] and "Fondo de Investi-gaciones Sanitarias, Instituto de Salud Carlos III", Spain [PI19/00819, co-funded by European Regional Development Fund/European Social Fund, "Investing in your future"]; Spanish Ministry of Economy, Industry and Competitiveness [SAF2016-75197-R]; "Junta de Castilla y Leon" [SA074P20]; AECC Scientific Foundation (2017/2020), Spain; "Proyectos de Investigación. Modalidad C2", University of Salamanca [18.K137/463AC01 and 18.K140/463AC01]; "Centro Internacional sobre el Envejecimiento" [OLD-HEPAMARKER, 0348_CIE_6_E], Spain and Fundación University of Salamanca, Spain [PC-TCUE18-20_051]; Fundació Marato TV3 [Ref. 201916-31]. Juan Cordoba Fellowship from the Spanish Association for the Study of the Liver [Fellowship Grant 2021 (AEHH)]. The funders had no role in study design, data collection and analysis, decision to publish, or preparation of the manuscript.

References

1. Masoodi M, Gastaldelli A, Hyötyläinen T, Arretxe E, Alonso C, Gaggini M, et al. Metabolomics and lipidomics in NAFLD: biomarkers and non-invasive diagnostic tests. Nat Rev Gastroenterol Hepatol. 2021;18:835–56.
2. Kalas MA, Chavez L, Leon M, Taweesedt PT, Surani S. Abnormal liver enzymes: a review for clinicians. World J Hepatol. 2021;13:1688–98.
3. Pugh RNH, Murray-Lyon IM, Dawson JL, Pietroni MC, Williams R. Transection of the oesophagus for bleeding oesophageal varices. Br J Surg. 1973;60:646–9.
4. Malinchoc M, Kamath PS, Gordon FD, Peine CJ, Rank J, ter Borg PCJ. A model to predict poor survival in patients undergoing transjugular intrahepatic portosystemic shunts. Hepatology. 2000;31:864–71.
5. Tulchinsky M, Colletti PM, Allen TW. Hepatobiliary scintigraphy in acute cholecystitis. Semin Nucl Med. 2012;42:84–100.
6. Chang HY, Liu B, Wang YZ, Wang WJ, Wang W, Li D, et al. Percutaneous transhepatic cholangiography *versus* endoscopic retrograde cholangiography for the pathological diagnosis of suspected malignant bile duct strictures. Medicine (Baltimore). 2020;99:e19545.
7. Voegeli DR, Crummy AB, Weese JL. Percutaneous transhepatic cholangiography, drainage, and biopsy in patients with malignant biliary obstruction. An alternative to surgery. Am J Surg. 1985;150:243–7.
8. Lambie H, Cook AM, Scarsbrook AF, Lodge JPA, Robinson PJ, Chowdhury FU. Tc^{99m}-hepatobiliary iminodiacetic acid (HIDA) scintigraphy in clinical practice. Clin Radiol. 2011;66:1094–105.
9. Rassam F, Olthof PB, Richardson H, van Gulik TM, Bennink RJ. Practical guidelines for the use of technetium-99m mebrofenin hepatobiliary scintigraphy in the quantitative assessment of liver function. Nucl Med Commun. 2019;40:297–307.

10. Ørntoft NW, Munk OL, Frisch K, Ott P, Keiding S, Sørensen M. Hepatobiliary transport kinetics of the conjugated bile acid tracer ^{11}C-CSar quantified in healthy humans and patients by positron emission tomography. J Hepatol. 2017;67:321–7.
11. Sigrist RMS, Liau J, Kaffas AE, Chammas MC, Willmann JK. Ultrasound elastography: review of techniques and clinical applications. Theranostics. 2017;7:1303–29.
12. Ferraioli G, Soares Monteiro LB. Ultrasound-based techniques for the diagnosis of liver steatosis. World J Gastroenterol. 2019;25:6053–62.
13. Ferraioli G, Meloni MF. Contrast-enhanced ultrasonography of the liver using SonoVue. Ultrasonography. 2018;37:25–35.
14. Shiina T, Nightingale KR, Palmeri ML, Hall TJ, Bamber JC, Barr RG, et al. WFUMB guidelines and recommendations for clinical use of ultrasound elastography: part 1: basic principles and terminology. Ultrasound Med Biol. 2015;41:1126–47.
15. Do RKG, Rusinek H, Taouli B. Dynamic contrast-enhanced MR imaging of the liver: current status and future directions. Magn Reson Imaging Clin N Am. 2009;17:339–49.
16. Manduca A, Bayly PJ, Ehman RL, Kolipaka A, Royston TJ, Sack I, et al. MR elastography: principles, guidelines, and terminology. Magn Reson Med. 2021;85:2377–90.
17. Nadarevic T, Giljaca V, Colli A, Fraquelli M, Casazza G, Miletic D, et al. Computed tomography for the diagnosis of hepatocellular carcinoma in adults with chronic liver disease. Cochrane Database Syst Rev. 2021;CD013362.
18. De Gaetano AM, Rufini V, Castaldi P, Gatto AM, Filograna L, Giordano A, et al. Clinical applications of ^{18}F-FDG PET in the management of hepatobiliary and pancreatic tumors. Abdom Imaging. 2012;37:983–1003.
19. Negrin JA, Zanzi I, Margouleff D. Hepatobiliary scintigraphy after biliary tract surgery. Semin Nucl Med. 1995;25:28–35.
20. Gupta M, Choudhury PS, Singh S, Hazarika D. Liver functional volumetry by Tc-99m mebrofenin hepatobiliary scintigraphy before major liver resection: a game changer. Indian J Nucl Med. 2018;33:277–83.
21. Stockmann M, Lock JF, Malinowski M, Niehues SM, Seehofer D, Neuhaus P. The LiMAx test: a new liver function test for predicting postoperative outcome in liver surgery. HPB (Oxford). 2010;12:139–46.
22. Cammann S, Oldhafer F, Ringe KI, Ramackers W, Timrott K, Kleine M, et al. Use of the liver maximum function capacity test (LiMAx) for the management of liver resection in cirrhosis - a case of hypopharyngeal cancer liver metastasis. Int J Surg Case Rep. 2017;39:140–4.
23. Sánchez-Fernández P, Martínez-Ordaz JL, Sánchez-Reyes K, Ferat-Osorio E. Usefulness of hepatobiliary scintigraphy in the follow-up of patients with biliary reconstruction. Rev Med Inst Mex Seguro Soc. 2015;53:538–45. Spanish.
24. van Roekel C, Reinders MTM, van der Velden S, Lam MGEH, Braat MNGJA. Hepatobiliary imaging in liver-directed treatments. Semin Nucl Med. 2019;49:227–36.
25. Foley WD, Jochem RJ. Computed tomography. Focal and diffuse liver disease. Radiol Clin North Am. 1991;29:1213–33.
26. Stephens DH, Sheedy PF, Hattery RR, MacCarty RL. Computed tomography of the liver. AJR Am J Roentgenol. 1977;128:579–90.
27. Tamm EP, Silverman PM. "Computed tomography of the liver"—a commentary. AJR Am J Roentgenol. 2006;186:1217–9.
28. Marolf AJ. Diagnostic imaging of the hepatobiliary system: an update. Vet Clin North Am Small Anim Pract. 2017;47:555–68.
29. Tsurusaki M, Sofue K, Hori M, Sasaki K, Ishii K, Murakami T, et al. Dual-energy computed tomography of the liver: uses in clinical practices and applications. Diagnostics (Basel). 2021;11:161.
30. Sharma B, Martin A, Zerizer I. Positron emission tomography-computed tomography in liver imaging. Semin Ultrasound CT MR. 2013;34:66–80.
31. O'Neill EK, Cogley JR, Miller FH. The ins and outs of liver imaging. Clin Liver Dis. 2015;19:99–121.

32. Vallejo Desviat P, Martínez De Vega V, Recio Rodríguez M, Jiménez De La Peña M, Carrascoso Arranz J. Diffusion MRI in the study of hepatic lesions. Cir Esp. 2013;91:9–16. Spanish.
33. Idilman IS, Li J, Yin M, Venkatesh SK. MR elastography of liver: current status and future perspectives. Abdom Radiol (NY). 2020;45:3444–62.
34. Korc P, Sherman S. ERCP tissue sampling. Gastrointest Endosc. 2016;84:557–71.
35. Iwashita T, Doi S, Yasuda I. Endoscopic ultrasound-guided biliary drainage: a review. Clin J Gastroenterol. 2014;7:94–102.
36. Salerno R, Davies SEC, Mezzina N, Ardizzone S. Comprehensive review on EUS-guided biliary drainage. World J Gastrointest Endosc. 2019;11:354–64.
37. Li Z, Li TF, Ren JZ, Li WC, Ren JL, Shui SF, et al. Value of percutaneous transhepatic cholangiobiopsy for pathologic diagnosis of obstructive jaundice: analysis of 826 cases. Acta Radiol. 2017;58:3–9.
38. Mohkam K, Malik Y, Derosas C, Isaac J, Marudanayagam R, Mehrzad H, et al. Percutaneous transhepatic cholangiographic endobiliary forceps biopsy *versus* endoscopic ultrasound fine needle aspiration for proximal biliary strictures: a single-centre experience. HPB. 2017;19:530–7.
39. Fohlen A, Bazille C, Menahem B, Jegonday MA, Dupont B, Le Pennec V, et al. Transhepatic forceps biopsy combined with biliary drainage in obstructive jaundice: safety and accuracy. Eur Radiol. 2019;29:2426–35.
40. Hayat U, Bakker C, Dirweesh A, Khan MY, Adler DG, Okut H, et al. EUS-guided *versus* percutaneous transhepatic cholangiography biliary drainage for obstructed distal malignant biliary strictures in patients who have failed endoscopic retrograde cholangiopancreatography: a systematic review and meta-analysis. Endosc Ultrasound. 2022;11:4–16.
41. Mirizzi PL. Operative cholangiography. Rev Esp Enferm Apar Dig Nutr. 1950;9:306–8. Spanish.
42. Balachandran S, Nealon WH, Goodman P. Operative cholangiography performed during laparoscopic cholecystectomy. Semin Ultrasound CT MR. 1993;14:325–30.
43. Lim SH, Tan HTA, Shelat VG. Comparison of indocyanine green dye fluorescent cholangiography with intra-operative cholangiography in laparoscopic cholecystectomy: a meta-analysis. Surg Endosc. 2021;35:1511–20.
44. Papagiannopoulou D. Technetium-99m radiochemistry for pharmaceutical applications. J Labelled Comp Radiopharm. 2017;60:502–20.
45. Huang X, Chen Y, Shao M, Li C, Zhang A, Dong J, et al. The value of ^{99m}Tc-labeled galactosyl human serum albumin single-photon emission computerized tomography/computed tomography on regional liver function assessment and posthepatectomy failure prediction in patients with hilar cholangiocarcinoma. Nucl Med Commun. 2020;41:1128–35.
46. Labeur TA, Cieslak KP, Van Gulik TM, Takkenberg RB, van der Velden S, Lam MGEH, et al. The utility of ^{99m}Tc-mebrofenin hepatobiliary scintigraphy with SPECT/CT for selective internal radiation therapy in hepatocellular carcinoma. Nucl Med Commun. 2020;41:740–9.
47. Wang H, Cao Y. Spatially resolved assessment of hepatic function using ^{99m}Tc-IDA SPECT. Med Phys. 2013;40:092501.
48. Markowicz-Piasecka M, Dębski P, Mikiciuk-Olasik E, Sikora J. Synthesis and biocompatibility studies of new iminodiacetic acid derivatives. Molecules. 2017;22:2265.
49. Yon M, Billotey C, Marty JD. Gadolinium-based contrast agents: from gadolinium complexes to colloidal systems. Int J Pharm. 2019;569:118577.
50. Ye F, Liu J, Ouyang H. Gadolinium ethoxybenzyl diethylenetriamine pentaacetic acid (Gd-EOB-DTPA)-enhanced magnetic resonance imaging and multidetector-row computed tomography for the diagnosis of hepatocellular carcinoma: a systematic review and meta-analysis. Medicine (Baltimore). 2015;94:e1157.
51. Shimada S, Kamiyama T, Kakisaka T, Orimo T, Nagatsu A, Asahi Y, et al. Impact of gadolinium-ethoxybenzyl-diethylenetriamine pentaacetic acid-enhanced magnetic resonance imaging on the prognosis of hepatocellular carcinoma after surgery. JGH Open. 2020;5:41–9.
52. Welle CL, Guglielmo FF, Venkatesh SK. MRI of the liver: choosing the right contrast agent. Abdom Radiol (NY). 2020;45:384–92.

53. Feng Q, Guan S, Zhao JR, Zhao XY, Zhang CC, Wang L, et al. Gadobenate dimeglumine-enhanced magnetic resonance imaging can accurately predict the severity of esophageal varices and portal vein pressure in patients with hepatitis B cirrhosis. J Dig Dis. 2020;21:104–11.
54. Liu C, Sun Y, Yang Y, Feng Y, Xie X, Qi L, et al. Gadobenate dimeglumine-enhanced biliary imaging from the hepatobiliary phase can predict progression in patients with liver cirrhosis. Eur Radiol. 2021;31:5840–50.
55. Delbeke D, Martin WH, Sandler MP, Chapman WC, Wright JK Jr, Pinson CW. Evaluation of benign *vs* malignant hepatic lesions with positron emission tomography. Arch Surg. 1998;133:510–6.
56. He YX, Guo QY. Clinical applications and advances of positron emission tomography with fluorine-18-fluorodeoxyglucose (^{18}F-FDG) in the diagnosis of liver neoplasms. Postgrad Med J. 2008;84:246–51.
57. Tan GJS, Berlangieri SU, Lee ST, Scott AM. FDG PET/CT in the liver: lesions mimicking malignancies. Abdom Imaging. 2014;39:187–95.
58. Ben-Haim S, Ell P. ^{18}F-FDG PET and PET/CT in the evaluation of cancer treatment response. J Nucl Med. 2009;50:88–99.
59. Almuhaideb A, Papathanasiou N, Bomanji J. ^{18}F-FDG PET/CT imaging in oncology. Ann Saudi Med. 2011;31:3–13.
60. Georgakopoulos A, Pianou N, Kelekis N, Chatziioannou S. Impact of ^{18}F-FDG PET/CT on therapeutic decisions in patients with colorectal cancer and liver metastases. Clin Imaging. 2013;37:536–41.
61. Lee SM, Kim HS, Lee S, Lee JW. Emerging role of ^{18}F-fluorodeoxyglucose positron emission tomography for guiding management of hepatocellular carcinoma. World J Gastroenterol. 2019;25:1289–306.
62. Weber WA, Ziegler SI, Thödtmann R, Hanauske AR, Schwaiger M. Reproducibility of metabolic measurements in malignant tumors using FDG PET. J Nucl Med. 1999;40:1771–7.
63. Fletcher JW, Djulbegovic B, Soares HP, Siegel BA, Lowe VJ, Lyman GH, et al. Recommendations on the use of ^{18}F-FDG PET in oncology. J Nucl Med. 2008;49:480–508.
64. Lee JW, Paeng JC, Kang KW, Kwon HW, Suh KS, Chung JK, et al. Prediction of tumor recurrence by ^{18}F-FDG PET in liver transplantation for hepatocellular carcinoma. J Nucl Med. 2009;50:682–7.
65. Sørensen M, Mikkelsen KS, Frisch K, Bass L, Bibby BM, Keiding S. Hepatic galactose metabolism quantified in humans using 2-^{18}F-fluoro-2-deoxy-*D*-galactose PET/CT. J Nucl Med. 2011;52:1566–72.
66. Keiding S, Sørensen M, Frisch K, Gormsen LC, Munk OL. Quantitative PET of liver functions. Am J Nucl Med Mol Imaging. 2018;8:73–85.
67. Khan MA, Combs CS, Brunt EM, Lowe VJ, Wolverson MK, Solomon H, et al. Positron emission tomography scanning in the evaluation of hepatocellular carcinoma. J Hepatol. 2000;32:792–7.
68. Yoon KT, Kim JK, Kim DY, Ahn SH, Lee JD, Yun M, et al. Role of ^{18}F-fluorodeoxyglucose positron emission tomography in detecting extrahepatic metastasis in pretreatment staging of hepatocellular carcinoma. Oncology. 2007;72:104–10.
69. Sørensen M, Frisch K, Bender D, Keiding S. The potential use of 2-[^{18}F]fluoro-2-deoxy-*D*-galactose as a PET/CT tracer for detection of hepatocellular carcinoma. Eur J Nucl Med Mol Imaging. 2011;38:1723–31.
70. Bak-Fredslund KP, Keiding S, Villadsen GE, Kramer S, Schlander S, Sørensen M. [^{18}F]-Fluoro-2-deoxy-*D*-galactose positron emission tomography/computed tomography as complementary imaging tool in patients with hepatocellular carcinoma. Liver Int. 2020;40:447–55.
71. Horsager J, Bak-Fredslund K, Larsen LP, Villadsen GE, Bogsrud TV, Sørensen M. Optimal 2-[^{18}F]fluoro-2-deoxy-*D*-galactose PET/CT protocol for detection of hepatocellular carcinoma. EJNMMI Res. 2016;6:56.
72. Kołodziej M, Bober B, Saracyn M, Kamiński G. The role of PET/CT with ^{11}C-methionine in contemporary nuclear medicine. Wiad Lek. 2020;73:2076–9.
73. Singhal T, Narayanan TK, Jain V, Mukherjee J, Mantil J. ^{11}C-*L*-methionine positron emission tomography in the clinical management of cerebral gliomas. Mol Imaging Biol. 2008;10:1–18.
74. Lapa C, Garcia-Velloso MJ, Lückerath K, Samnick S, Schreder M, Otero PR, et al. ^{11}C-methionine-PET in multiple myeloma: a combined study from two different institutions. Theranostics. 2017;7:2956–64.
75. D'souza MM, Sharma R, Jaimini A, Saw SK, Singh D, Mondal A. Combined ^{18}F-FDG and ^{11}C-methionine PET/CT scans in a case of metastatic hepatocellular carcinoma. Indian J Nucl Med. 2014;29:171–4.

76. Harris SM, Davis JC, Snyder SE, Butch ER, Vavere AL, Kocak M, et al. Evaluation of the biodistribution of ^{11}C-methionine in children and young adults. J Nucl Med. 2013;54:1902–8.
77. Morales-Lozano MI, Viering O, Samnick S, Rodriguez-Otero P, Buck AK, Marcos-Jubilar M, et al. ^{18}F-FDG and ^{11}C-methionine PET/CT in newly diagnosed multiple myeloma patients: comparison of volume-based PET biomarkers. Cancers (Basel). 2020;12:1042.
78. Kuang Y, Salem N, Tian H, Kolthammer JA, Corn DJ, Wu C, et al. Imaging lipid synthesis in hepatocellular carcinoma with [methyl-^{11}C]choline: correlation with *in vivo* metabolic studies. J Nucl Med. 2011;52:98–106.
79. Dang YZ, Zhang DX, Wang GD, Zhao HL, Huang SG, Li J. Safety and efficacy of the metabolic profiling of the BIMRT utilizing ^{18}F FDG PET-CT. Technol Cancer Res Treat. 2020;19:1533033820960723.
80. Lee YH, Wu MR, Hsiao JK. Organic anion transporting polypeptide 1B1 is a potential reporter for dual MR and optical imaging. Int J Mol Sci. 2021;22:8797.
81. Portnoy E, Gurina M, Magdassi S, Eyal S. Evaluation of the near infrared compound indocyanine green as a probe substrate of p-glycoprotein. Mol Pharm. 2012;9:3595–601.
82. Namikawa T, Sato T, Hanazaki K. Recent advances in near-infrared fluorescence-guided imaging surgery using indocyanine green. Surg Today. 2015;45:1467–74.
83. Dutta HK, Rao DN, Gupta DK. Indocyanine green clearance test to evaluate liver function in rat model of extrahepatic biliary atresia. Afr J Paediatr Surg. 2018;15:5–9.
84. Schwarz C, Plass I, Fitschek F, Punzengruber A, Mittlböck M, Kampf S, et al. The value of indocyanine green clearance assessment to predict postoperative liver dysfunction in patients undergoing liver resection. Sci Rep. 2019;9:8421.
85. Wakabayashi T, Cacciaguerra AB, Abe Y, Bona ED, Nicolini D, Mocchegiani F, et al. Indocyanine green fluorescence navigation in liver surgery: a systematic review on dose and timing of administration. Ann Surg. 2022;275:1025–34.
86. Purich K, Dang JT, Poonja A, Sun WYL, Bigam D, Birch D, et al. Intraoperative fluorescence imaging with indocyanine green in hepatic resection for malignancy: a systematic review and meta-analysis of diagnostic test accuracy studies. Surg Endosc. 2020;34:2891–903.
87. Qi C, Zhang H, Chen Y, Su S, Wang X, Huang X, et al. Effectiveness and safety of indocyanine green fluorescence imaging-guided hepatectomy for liver tumors: a systematic review and first meta-analysis. Photodiagnosis Photodyn Ther. 2019;28:346–53.
88. Hu Y, Fu T, Zhang Z, Hua L, Zhao Q, Zhang W. Does application of indocyanine green fluorescence imaging enhance clinical outcomes in liver resection? A meta-analysis. Photodiagnosis Photodyn Ther. 2021;36:102554.
89. Majlesara A, Golriz M, Hafezi M, Saffari A, Stenau E, Maier-Hein L, et al. Indocyanine green fluorescence imaging in hepatobiliary surgery. Photodiagnosis Photodyn Ther. 2017;17:208–15.
90. Zhang YM, Shi R, Hou JC, Liu ZR, Cui ZL, Li Y, et al. Liver tumor boundaries identified intraoperatively using real-time indocyanine green fluorescence imaging. J Cancer Res Clin Oncol. 2017;143:51–8.
91. Osayi SN, Wendling MR, Drosdeck JM, Chaudhry UI, Perry KA, Noria SF, et al. Near-infrared fluorescent cholangiography facilitates identification of biliary anatomy during laparoscopic cholecystectomy. Surg Endosc. 2015;29:368–75.
92. Kramer W, Wess G. Bile acid transport systems as pharmaceutical targets. Eur J Clin Invest. 1996;26:715–32.
93. Ørntoft NW, Gormsen LC, Keiding S, Munk OL, Ott P, Sørensen M. Hepatic bile acid transport increases in the postprandial state: a functional ^{11}C-CSar PET/CT study in healthy humans. JHEP Rep. 2021;3:100288.
94. Schacht AC, Sørensen M, Munk OL, Frisch K. Radiosynthesis of *N*-^{11}C-methyl-taurine-conjugated bile acids and biodistribution studies in pigs by PET/CT. J Nucl Med. 2016;57:628–33.
95. Testa A, Dall'Angelo S, Mingarelli M, Augello A, Schweiger L, Welch A, et al. Design, synthesis, *in vitro* characterization and preliminary imaging studies on fluorinated bile acid derivatives as PET tracers to study hepatic transporters. Bioorg Med Chem. 2017;25:963–76.

96. Chong HS, Chen Y, Kang CS, Sun X, Wu N. Novel ^{64}Cu-radiolabeled bile acid conjugates for targeted PET imaging. Bioorg Med Chem Lett. 2015;25:1082–5.
97. Blazquez AG, Briz O, Romero MR, Rosales R, Monte MJ, Vaquero J, et al. Characterization of the role of ABCG2 as a bile acid transporter in liver and placenta. Mol Pharmacol. 2012;81:273–83.
98. Mendoza ME, Monte MJ, Serrano MA, Pastor-Anglada M, Stieger B, Meier PJ, et al. Physiological characteristics of *allo*-cholic acid. J Lipid Res. 2003;44:84–92.
99. Leuenberger M, Häusler S, Höhn V, Euler A, Stieger B, Lochner M. Characterization of novel fluorescent bile salt derivatives for studying human bile salt and organic anion transporters. J Pharmacol Exp Ther. 2021;377:346–57.
100. Rohacova J, Marin ML, Martínez-Romero A, O'Connor JE, Gomez-Lechon MJ, Donato MT, et al. Photophysical characterization and flow cytometry applications of cholylamidofluorescein, a fluorescent bile acid scaffold. Photochem Photobiol Sci. 2008;7:860–6.
101. Annaert P, Ye ZW, Stieger B, Augustijns P. Interaction of HIV protease inhibitors with OATP1B1, 1B3, and 2B1. Xenobiotica. 2010;40:163–76.
102. Monte MJ, Rosales R, Macias RI, Iannota V, Martinez-Fernandez A, Romero MR, et al. Cytosol-nucleus traffic and colocalization with FXR of conjugated bile acids in rat hepatocytes. Am J Physiol Gastrointest Liver Physiol. 2008;295:G54–62.
103. Monte MJ, Dominguez S, Palomero MF, Macias RI, Marin JJG. Further evidence of the usefulness of bile acids as molecules for shuttling cytostatic drugs toward liver tumors. J Hepatol. 1999;31:521–8.
104. Lozano E, Monte MJ, Briz O, Hernández-Hernández A, Banales JM, Marin JJG, et al. Enhanced antitumour drug delivery to cholangiocarcinoma through the apical sodium-dependent bile acid transporter (ASBT). J Control Release. 2015;216:93–102.
105. Milkiewicz P, Mills CO, Hubscher SG, Cardenas R, Cardenas T, Williams A, et al. Visualization of the transport of primary and secondary bile acids across liver tissue in rats: *in vivo* study with fluorescent bile acids. J Hepatol. 2001;34:4–10.
106. Milkiewicz P, Baiocchi L, Mills CO, Ahmed M, Khalaf H, Keogh A, et al. Plasma clearance of cholyl-lysyl-fluorescein: a pilot study in humans. J Hepatol. 1997;27:1106–9.
107. Milkiewicz P, Saksena S, Cardenas T, Mills CO, Elias E. Plasma elimination of cholyl-lysyl-fluorescein (CLF): a pilot study in patients with liver cirrhosis. Liver. 2000;20:330–4.
108. Mills CO, Milkiewicz P, Saraswat V, Elias E. Cholyllysyl fluroscein and related lysyl fluorescein conjugated bile acid analogues. Yale J Biol Med. 1997;70:447–57.
109. Barber JA, Stahl SH, Summers C, Barrett G, Park BK, Foster JR, et al. Quantification of drug-induced inhibition of canalicular cholyl-*l*-lysyl-fluorescein excretion from hepatocytes by high content cell imaging. Toxicol Sci. 2015;148:48–59.
110. Vartak N, Guenther G, Joly F, Damle-Vartak A, Wibbelt G, Fickel J, et al. Intravital dynamic and correlative imaging of mouse livers reveals diffusion-dominated canalicular and flow-augmented ductular bile flux. Hepatology. 2021;73:1531–50.
111. Crawford JM, Lin YJ, Teicher BA, Narciso JP, Gollan JL. Physical and biological properties of fluorescent dansylated bile salt derivatives: the role of steroid ring hydroxylation. Biochim Biophys Acta. 1991;1085:223–34.
112. Rohacova J, Sastre G, Marin ML, Miranda MA. Dansyl labeling to modulate the relative affinity of bile acids for the binding sites of human serum albumin. J Phys Chem B. 2011;115:10518–24.
113. Filipe HAL, Pokorná Š, Hof M, Amaro M, Loura LMS. Orientation of nitro-group governs the fluorescence lifetime of nitrobenzoxadiazole (NBD)-labeled lipids in lipid bilayers. Phys Chem Chem Phys. 2019;21:1682–8.
114. Rohacova J, Marín ML, Martinez-Romero A, Diaz L, O'Connor JE, Gomez-Lechon MJ, et al. Fluorescent benzofurazan-cholic acid conjugates for *in vitro* assessment of bile acid uptake and its modulation by drugs. ChemMedChem. 2009;4:466–72.